Materials for Renewable and Sustainable Energy (2018) 7:14
https://doi.org/10.1007/s40243-018-0121-0

ORIGINAL PAPER

Influence of Ni–Al coating thickness on spectral selectivity and thermal performance of parabolic trough collector

Tawat Suriwong[1] · Chanon Bunmephiphit[2] · Warisa Wamae[1] · Sathit Banthuek[1]

Received: 13 February 2018 / Accepted: 14 May 2018 / Published online: 19 May 2018

Abstract

This study investigates the influence of Ni–Al coating thickness on the spectral selectivity and thermal performance of a parabolic trough collector (PTC). Three thicknesses of Ni–Al coating for use as solar absorber material were successfully prepared on the outer surface of a stainless steel 316L (SS) tube by flame spray. The phase, morphology, and reflectance (R) of the Ni–Al coatings were characterized using several techniques. The PTC and solar receiver tube were specially designed and constructed for observing the collector thermal performance by following ASHRAE 93-1986. Looking at the results, the actual average thicknesses of the three Ni–Al coatings turn out to be 195, 215, and 299 µm. The morphology and chemical composition of all three thicknesses are similar. The chemical composition in the cross-sectional view exhibits non-uniform distribution. The three thicknesses of the coating are composed of NiO and Al_2O_3 phases, which also corresponded to the results of SEM–EDX mapping. The differences in a solar absorptance (α) of the three thicknesses of Ni–Al coating are not statistically significant, with an average α value of 0.74–0.75. However, there are differences in thermal efficiency of the PTC depending on the thickness of the Ni–Al coating. Of the three samples, the thickest one (299 µm) demonstrates the highest ability to convert solar radiation into thermal energy.

Keywords Ni–Al · Solar absorber · Solar absorptance · Thermal performance · Parabolic trough collector (PTC)

Introduction

One type of linear concentrating solar collector is the parabolic trough collector (PTC) which is useful in a wide range of applications where the working temperatures are 50–400 °C [1]. In essence, a PTC consists of a parabolic trough mirror or reflector and a solar receiver tube in the focal line of the reflector. Sunlight falls on the reflector, which focuses it onto the solar receiver tube. The outer surface of the solar receiver tube is coated with solar selective materials to absorb that concentrated sunlight and also any sunlight that falls directly on the tube itself. All the collected radiation is then converted into thermal energy [2, 3]. One important task is the development of a solar selective absorber to achieve high solar absorptance (α) or low reflectance (R) over the whole range of the solar spectrum (300–2500 nm) and low emittance (ε) of long wavelength infrared (IR) radiation at 2.5–20 µm [4–6].

At present, there are several coatings that have been used as solar selective absorbers for high-temperature operation of PTC: Pt–Al_2O_3, W–Al_2O_3, Mo–Al_2O_3, AlNi–Al_2O_3, Au–MgO, Mo–SiO_2, Ni–SiO_2, TiAlN/TiAlON/Si_3N_4, TiAlN/TiAlON/SiO_2, HfMoN/HfON/Al_2O_3, $NiCo_2O_4$, $CuCoO_4$ (NiFe)Co_2O_5, Ni-25 graphite and Ni-5Al [4, 6–10]. In addition, the solar absorber Ni–5Al has attracted considerable attention as a solar selective coating for concentrating solar radiation at high operating temperatures [10]. Ni–Al composite coatings are particularly applied to numerous special applications that required a high melting point, low-density (5890 kg m^{-3}), high thermal conductivity, excellent anticorrosion, high-temperature oxidation, high thermal stability, and high-temperature mechanical properties [11–13]. A previous study by this researcher has successfully prepared Ni–Al solar absorber using a flame spray technique, especially, the α of the Ni–Al solar absorber was 0.77 [14]. However, the effect of Ni–Al coating thickness on spectral

✉ Tawat Suriwong
tawats@nu.ac.th

[1] School of Renewable Energy Technology, Naresuan University, Phitsanulok 65000, Thailand

[2] Rattanakosin College for Sustainable Energy and Environment, Rajamangala University of Technology Rattanakosin, Nakhon Pathom 73170, Thailand

selectivity and thermal performance of PTC is uncertain at present, and further research in this area is necessary.

In the present study, various thicknesses of Ni–Al coating onto an outer surface of stainless steel tube were prepared by flame spray technique. The effect of the coating thickness on spectral selectivity, including the solar absorptance (α) and thermal emittance (ε), was investigated. The coated tube was then installed into a specially designed PTC, and the influence of coating thickness on thermal performance was determined.

Experiment

Preparation and characterization of Ni–Al coatings

Commercial Ni-5wt% Al powder (450 NS, Oerlikon, Metco, Switzerland) with the spherical shape and size distribution of 45–90 µm was used as a starting material. A stainless steel 316L (SS) tube with inner diameter 27.9 mm, outer diameter 33.33 mm, and length 1000 mm was prepared for later installation as a receiver tube in PTC. To prepare the tube, the Ni-5wt% Al powder was coated onto the outer surface of the SS tube using CastoDyn DS 8000 flame spray equipment (Castolin Eutectic, Switzerland). The flame spray setup and fuel condition for the coating process were previously proposed [14]. The variation of Ni–Al coating thickness was carried out by the flame spray process for 120, 180, and 300 s under the same conditions. These three Ni–Al coatings were characterized to determine their morphology, chemical composition, and phase, using a scanning electron microscope (SEM, JEOL JSM-5910LV) equipped with an energy-dispersive X-ray (EDX) analyzer, an X-ray diffractometer (XRD, PANalytical) with Cu–K_α radiation in the range of 20–80°. The spectral reflectance (R) was measured using a UV–Vis-NIR spectrophotometer (UV-3101PC, Shimadzu) in the range of 300–2500 nm at room temperature and a Fourier transform infrared spectrophotometer (FTIR, Bruker Tensor 27) in the wavelength of infrared region (2500–25,000 nm). The spectral selectivity of the coatings is explained in terms of the spectral R in the wavelength range of the UV–Vis-NIR and IR regions. The α was determined from the measured R spectrum, as expressed in Eq. (1) [14, 15],

$$\alpha = \frac{\int_{0.3\mu m}^{2.5\mu m} I_s(\lambda)(1 - R(\lambda))d\lambda}{\int_{0.3\mu m}^{2.5\mu m} I_s(\lambda)d\lambda}, \quad (1)$$

where $R(\lambda)$ is the observed reflectance spectrum of the coating at a specific wavelength of 300–2500 nm, and $I_s(\lambda)$ is the solar spectral irradiance at air mass (AM) 1.5 [16].

Design and manufacture of the PTC

PTCs are designed for hot water generation. A parabolic reflector was designed with the length (L) of 1 m and rim angle (φ_r) of 75° to decrease the collector's surface area, increase flexibility for fabricating a reflector material, and lower reflective material cost. The concentration ratio (C) is calculated from the ratio of the aperture area (A_a) to the receiver area (A_r), as shown in Eq. (2). In this PTC prototype, the C is fixed at 15.

$$C = \frac{A_a}{A_r} \quad (2)$$

The aperture width (W_a) of the parabolic trough can be calculated using Eq. (3), where D_{abs} is the outer diameter of the SS absorber tube (OD = 33.33 mm). So, W_a is equal to 1.57 m.

$$C = \frac{W_a}{\pi D_{abs}} \quad (3)$$

The focal distance (f) of this parabolic concentrator was 0.511 m, which is calculated by following Eq. (4). The focal line is very significant because the receiver tube is mounted precisely in this line.

$$W_a = 4f \tan\left(\frac{\phi_r}{2}\right) \quad (4)$$

The two-dimensional parabola equation of the parabolic concentrator is shown in Eq. (5). This equation is used to draw a diagram on paper to enable highly accurate design and construction of the parabolic reflector. The dimensions of the parabola trough are summarized in Table 1.

$$Y = \frac{1}{4f}X^2 = 0.4892X^2 \quad (5)$$

A parabolic trough was constructed of wood for its uniform thickness, light weight, and ease of use. The structure

Table 1 Dimensions of the parabolic trough and solar receiver tube for the PTC prototype

Descriptions	Dimension
Parabola length (L)	1.00 m
parabola aperture (W_a)	1.57 m
focal distance (f)	0.511 m
Rim angle (φ_r)	75°
Concentration ratio (C)	15
Outer diameter of absorber tube (D_{abs})	33.33 mm
Inner diameter of absorber tube	27.90 mm
Glass envelope tube diameter	65 mm
Glass envelope tube wall thickness	55 mm

was reinforced with fiberglass and coordinate resin to a thickness of 3 mm, to increase the strength, water resistance, damage from pollution and environmental stresses, resistance to wind, termites, and long-term stability [17]. The support of the reflector was made of fiberglass and coordinate resin with a smooth surface that is able to reflect the sunlight with accuracy. A very smooth metal sheet with a thickness of 1 mm was glued on top of the fiberglass surface.

A flexible reflective material in the form of a commercial polyethylene terephthalate (PET) film coated with reflecting aluminum, which is a self-adhesive sticker, with a thickness 0.1 mm and a reflecting rate $\geq 90\%$ (purchased from Benefit K&J associate Co., Ltd., Thailand), was used as a solar reflector. The PET reflector film was carefully mounted on the smooth surface of the metal sheet to maintain a precise solar reflection to the focal line along the parabolic trough.

The solar receiver tube is the most important part of the PTC due to its thermal and optical performance. This performance depends on the solar absorber materials, the prevention of heat loss by the glass envelope tube, the distance between the glass tube and the absorber tube, and the coating materials used on the absorber tube [2]. In this prototype, the solar receiver tube consists of a SS tube coated with three different thicknesses of Ni–Al coating. A glass envelope tube is fitted over the absorber tube. There is a vacuum between the absorber and the glass envelope tube. Coupling joints (made of Teflon) are used to fit the glass envelope tube at both ends to achieve an airtight enclosure and maintain a vacuum inside the solar receiver tube. This is one of the more complicated parts of the construction process. The vacuum is maintained to achieve a high amount of thermal energy in the absorber and to prevent heat loss.

Figure 1 shows all the components that are used to assemble the solar receiver tube. On one side of the coupling joint, a pneumatic fitting was connected for evacuating the space between the absorber tube and the glass envelope tube. In addition, Viton O-rings with a thermal stability of 350 °C were assembled inside of the coupling joints to prevent tension between the glass envelope tube and the solar absorber tube due to expansion at high-temperature. The solar receiver tube was evacuated to achieve a vacuum at 4.3 ± 1 kPa. The dimensions of the solar receiver tube in this prototype are summarized in Table 1.

A solar tracking system is required to enable the PTC to follow the sun (sun travels 15°/h). In this experiment, a manual solar tracker was installed in the PTC prototype. Because of its simple mechanism, the manual solar tracker is easy to assemble and economical for use in a pilot study for research purposes. The manual solar tracking system consists of a low speed 12 V DC motor with 5 rpm, a high-resolution camera, and an electronic controller. This equipment enhances accuracy while tracking the sun.

Testing the thermal performance of the PTC

In this study, the thermal performance of the PTC was investigated by following ASHRAE 93-1986 with an open-loop testing system in which water is supplied continuously, as shown in Fig. 2. The thermal performance test is evaluated by recording values of instantaneous thermal efficiency (η), which is calculated from several parameters such as inlet (T_i) and outlet (T_o) water temperature, ambient temperature

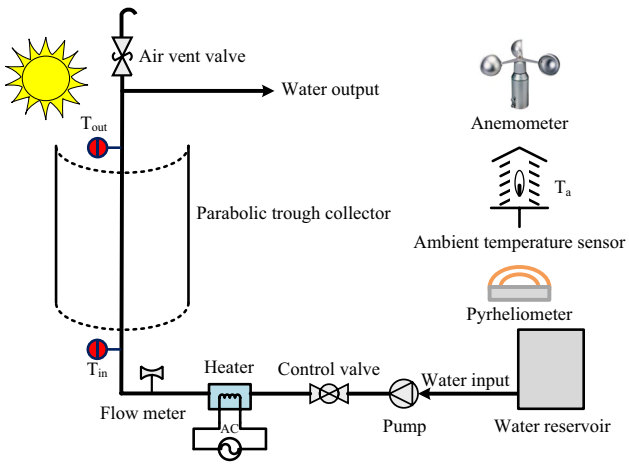

Fig. 2 The configuration of the thermal performance testing with an open-loop system following ASHRAE 93-1986

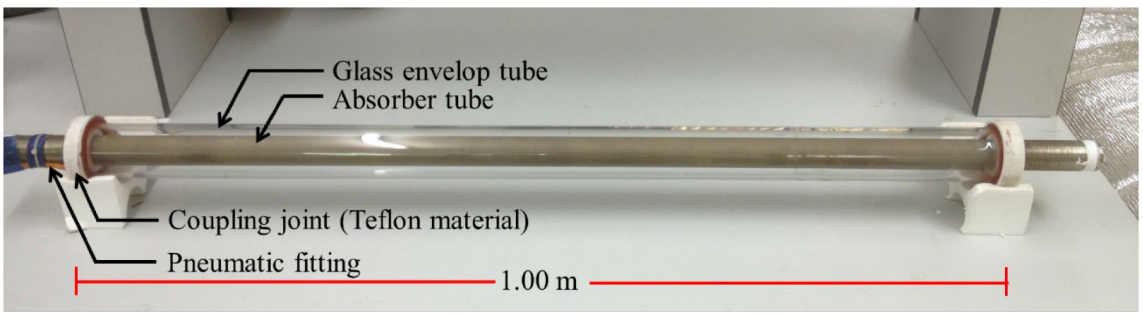

Fig. 1 The components of the solar receiver tube

(T_a), direct solar irradiance (I_d) and mass flow rate ($\dot{m}$). In addition, all parameters are performed under steady-state or quasi-steady-state conditions. In accordance with the ASHRAE 93-1986 standard, the inlet temperature and mass flow rate of the water were kept at a constant value before being supplied to the PTC, while the water outlet temperature is measured to calculate the useful energy gain (Q_u). The thermal efficiency (η) of a PTC operating under steady-state conditions can be expressed as follows:

$$\eta = F_R\eta_o - \frac{F_R U_L}{C}\left(\frac{T_i - T_a}{I_d}\right), \quad (6)$$

where F_R is the solar collector heat removal factor, η_o is the optical efficiency and U_L is the overall heat loss coefficient of the solar collector (W/m^2.^{o}C). With a PTC operating under steady-state conditions, the factors F_R, η_o and U_L are close to constant. Therefore, thermal efficiency equations (Eq. 6) can be plotted between η against the heat loss parameter $(T_i - T_a)/I_d$ as a straight line, indicating a linear relationship between η and $(T_i - T_a)/I_d$. The intercept on a vertical efficiency axis is $F_R\eta_o$, which is defined as a maximum of the collector efficiency if the T_i is equal to T_a. $-F_R U_L/C$ is a slope of the line, according to the efficiency difference divided by the corresponding horizontal scale difference. The small value of slope implies that a low heat loss from the PTC to the surrounding [18].

The PTC system with different thicknesses of Ni–Al coating as the solar absorber of the receiver tube was installed at a terrace of the Department of Physics, Faculty of Science, Naresuan University, Phitsanulok, Thailand, as shown in Fig. 3. The PTC was mounted in a north–south direction, tracking the sun from east to west. T_i and T_o of water were measured by a type K thermocouple and were recorded using a data recorder (AI 210, Wisco, Thailand) connected to a personal computer. T_a and I_d were recorded with an RTD sensor (PT-100-resistance temperature device) and a pyrheliometer at a meteorological station of the School of Renewable Energy Technology, Naresuan University, Phitsanulok, Thailand. Wind speed was measured by a vane and cup type anemometer.

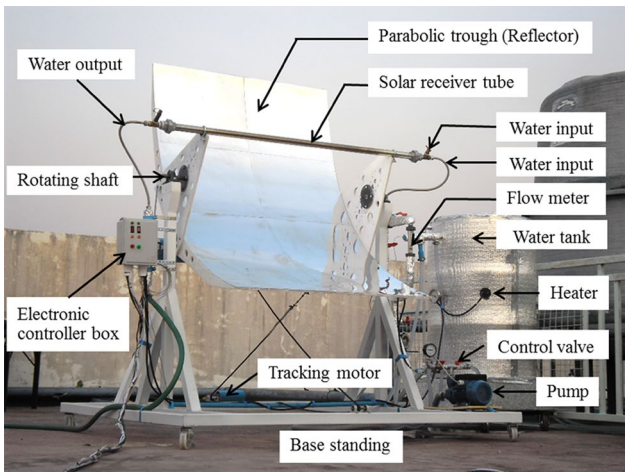

Fig. 3 The overview of the PTC prototype using different thicknesses of Ni-Al coating as the solar absorber of the receiver tube

Results and discussion

Cross-sectional SEM images of the three thicknesses of the Ni–Al coating are shown in Fig. 4a–c. These images show that the Ni–Al coatings were successfully prepared on the outer surface of SS tube using a flame spray technique and an available commercially raw material (Ni-5wt% Al particles). The Ni–Al coating is built up layer by layer as the result of the individual melted Ni and Al particles in the form of splat sprayed from a spray gun. This microstructure is similar to those of Ni–Al composite coatings prepared by other people using the same and other techniques [14, 19, 20]. However, it can be observed that the samples with different thicknesses have different pore sizes and interlamellar porosity. The pores occurred after cutting and polishing the samples, indicating that these areas had a low-density microstructure due to the weak bond between the melted Ni and Al particles. According to previous studies, this is caused by imperfectly melted and un-melted particles of raw materials during the flame spraying process [13, 14]. Moreover, there are cracks at the interface between the Ni–Al coating and the outer surface of the SS tube as the result of a residual stress from the thermal expansion mismatch between the coating and the SS tube. The three thicknesses of Ni–Al coatings are measured, and they have an average thickness of 195, 215 and 299 μm, as shown in Fig. 4a–c. It indicates that the thickness of Ni–Al coatings increases with increasing the spraying time. The SEM images of surface morphologies with various thicknesses of the samples are shown in Fig. 4d–f. The surfaces of all of the coatings have a dark gray color and are relatively rough. These rough surfaces are built up from the high velocity of melted Ni and Al particles forced onto the previous layer by high-pressure spray and temperature. It can be seen that the thickness of the Ni–Al coating layer has an insignificant effect on the degree of surface roughness.

To discuss the chemical distribution on the cross-section area of Ni–Al coatings, typical SEM and EDX mapping analyses are shown in Fig. 5. As seen on the SEM images, the Ni–Al coatings are overlapped by the splatter of melted Ni and Al particles. There are two contrasting regions, shown as light and dark areas, which can be used to identify the different phases. The EDX analyses show that the cross-section area of all Ni–Al coatings is composed of Ni, Al and

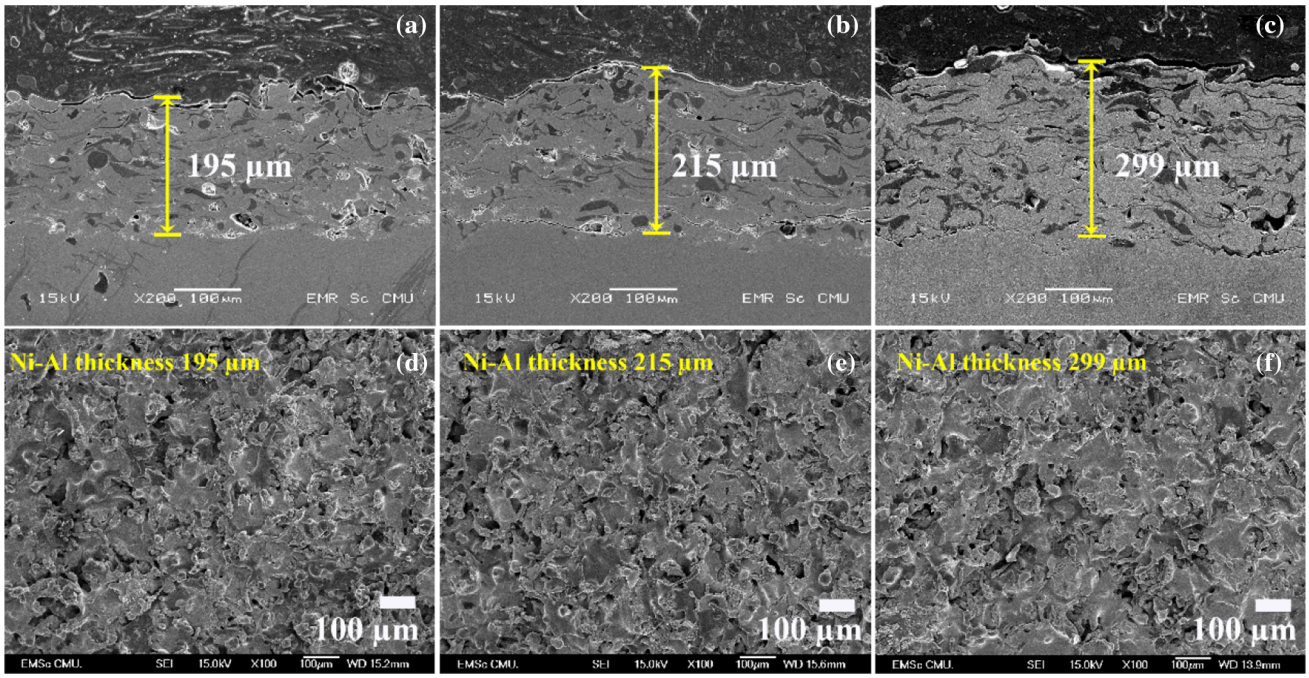

Fig. 4 SEM images of the cross-section (**a**–**c**) and surface (**d**–**f**) of the Ni–Al solar absorber with the three different thicknesses

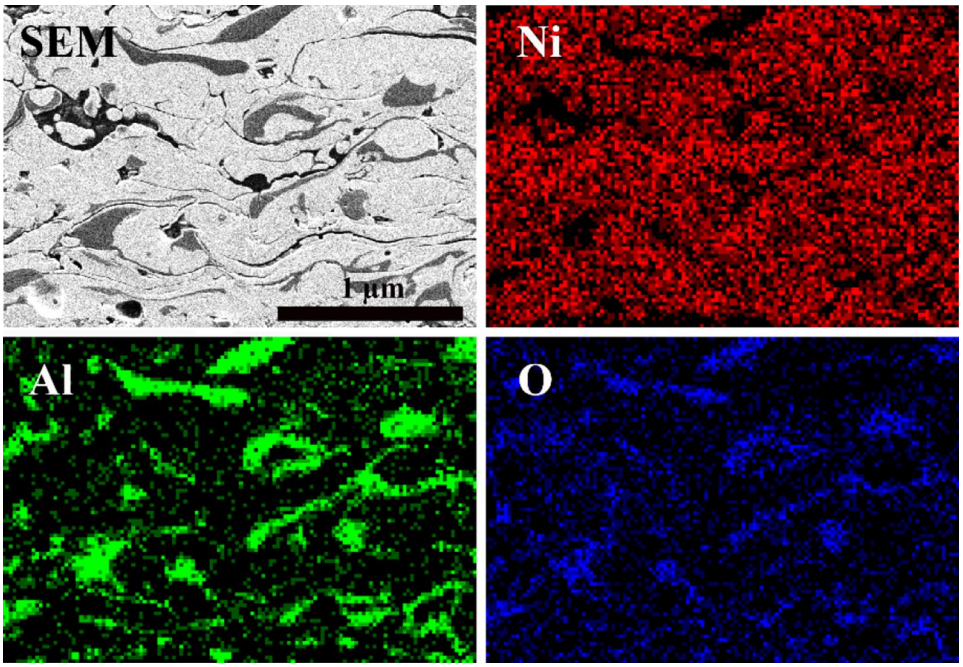

Fig. 5 SEM and EDX mapping analyses of the cross-sectional area of the Ni–Al coating

O elements with non-uniform distribution, corresponding to Ni-5wt%Al deposits prepared by air plasma spraying [19, 20]. The light gray and gray regions correspond to Ni and Al-rich areas, respectively. However, the O element more evenly distributes over the cross-section area of the sample. O appears to be distributed predominantly in the Al-rich area. As a result of the practical operation of a flame spray process in an open environment, the splatter of both melted Ni and Al particles react with oxygen gas during ejection from the spay gun to the outer surface of the SS tube and cooling process of the coating. The chemical composition of the fundamental elements on the cross-section area of this coating is Ni 80.26 wt%, Al 8.93 wt% and O 10.81 wt%. Regardless of the different thicknesses of Ni–Al coating,

it is found that microstructure, chemical distribution, and chemical composition turn out similarly. The SEM and EDX analyses confirm that all the thicknesses of the Ni–Al coating present non-homogeneous chemical distribution and consist of Ni, Al, and O elements.

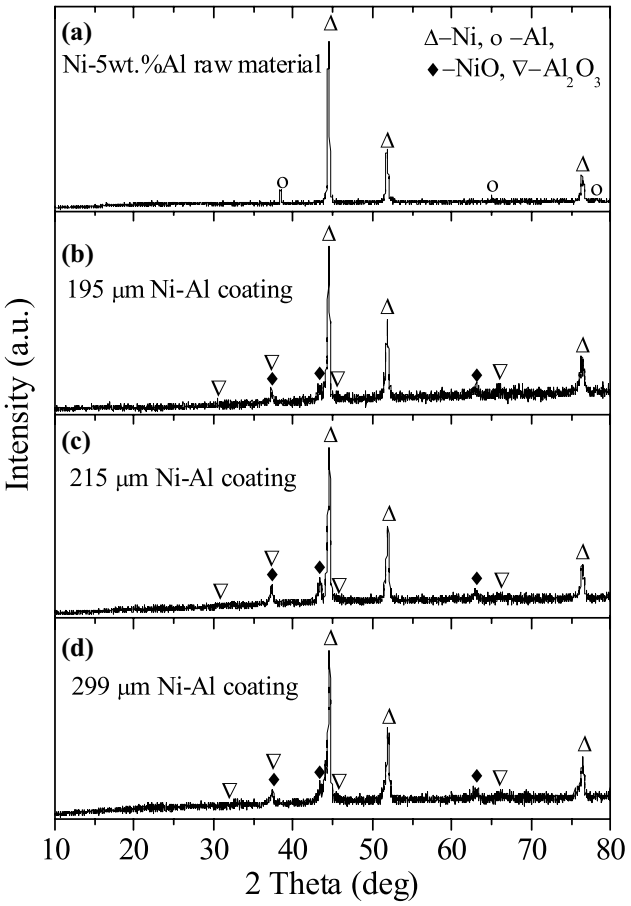

Fig. 6 The XRD pattern of **a** Ni-5wt%Al raw material, and **b**–**d** Ni–Al coating with different thicknesses of 195, 215 and 299 μm, respectively

To further investigate the phase phenomenon, the Ni–Al coating was characterized by XRD, and the resulting patterns are shown in Fig. 6. The observed XRD patterns are indexed and compared with Ni, Al, NiO and Al_2O_3 for the JCPDS database Nos. 4-0850, 01-85-1327, 1-1239, and 47-1292, respectively. As for the available commercial raw material which is produced by mixing Ni and Al powders together, the raw material is indexed as a combination of pure Ni and Al phases. In all the coating thicknesses, the coatings are composed of Ni, Al, NiO, and Al_2O_3 phases, according to previous studies [14, 19]. The NiO and Al_2O_3 phases are contained in the Ni–Al coating because of the splatter of melted Ni and Al particles oxidized with oxygen gas in the environment during flame spray operation, corresponding to the SEM-EXD result in Fig. 5. However, the NiAl, $AlNi_3$ or Al_3Ni_5 phases are not found in the Ni–Al solar absorber as a result of low Al content in this coating. This is in good agreement with the Ni–Al binary phase diagram [21].

Figure 7a shows the measured reflectance (R) spectra of the three different coating thicknesses, together with the spectral irradiance at AM 1.5. The R of all the coatings increases slightly with the increasing wavelength. The R is particularly low in the region of high spectral irradiance (400–1000 nm). Over the whole wavelength of the solar spectrum, the calculated solar absorptance (α) of the Ni–Al coating with the thicknesses of 199, 215, and 299 μm is 0.75, 0.74, and 0.75, respectively. These α values of the Ni–Al coatings are larger than those of Ni–5Al solar absorbers and related coatings such as Ni-25 graphite and WC-25 Ni prepared by the thermal spray technique without heat treatment for 6 h at 600 °C [10]. However, the α of this coating is relatively lower than those of commercial solar selective coatings that are prepared using advanced coating

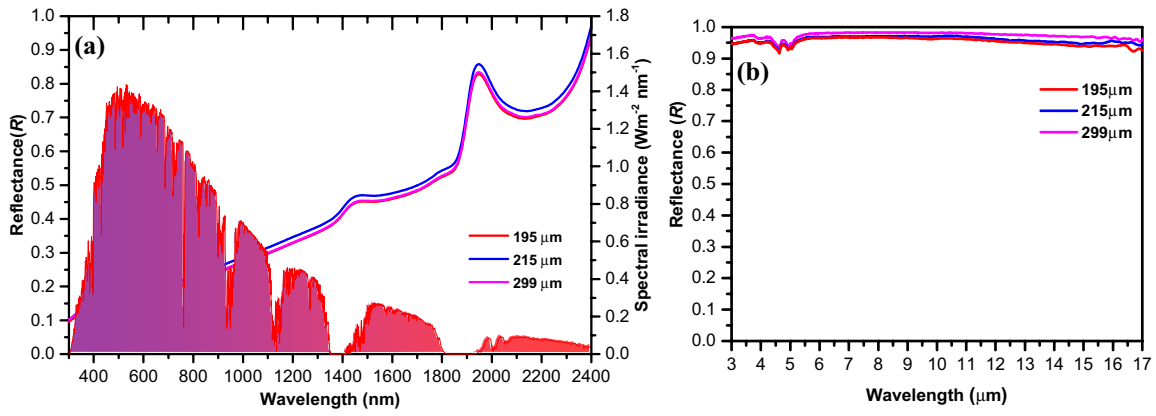

Fig. 7 The measured spectral reflectance (R) of the Ni–Al coatings with the three thicknesses in the wavelength of **a** UV–Vis-NIR regions, together with spectral irradiance at AM 1.8 and **b** the IR region

technology under vacuum conditions (sputtering, vacuum evaporation, chemical vapor deposition, and pulsed laser deposition) for the high operating temperature of solar thermal applications [5, 6]. Figure 5b shows the spectral R in the wavelength ranges of the IR region. The spectral R of the different coatings is all above 0.95 over the wavelength range of 3.0–17 μm. As can be seen in the results shown in Fig. 5, the different thicknesses of Ni–Al solar absorber prepared by the flame spray technique have an insignificant effect on spectral selectivity. The spectral R of all the Ni–Al coatings also corresponds to the theoretical property of the selective solar absorber materials.

Figure 8 shows the thermal efficiency curves of the PTC when using the different thicknesses of Ni–Al coating on the SS tube, as determined from a measurement based on the ASHRAE standard 93-1986. A thermal efficiency equation of each thickness of Ni–Al coating was calculated with a convenient mathematical tool of a linear least-squares fit established with 50 data points/thickness. As for the thermal efficiency equation, the intercepts ($F_R\eta_o$) are 0.295, 0.409, and 0.469 for Ni–Al coating thickness of 195, 219 and 299 μm, respectively. The slopes ($-F_RU_L/C$) of the three thicknesses are 1.732, 1.697 and 1.793, respectively.

To discuss the influence of Ni–Al coating thickness on PTC thermal performance in more detail, all parameters related to the thermal efficiency equation should be determined. Fundamentally, optical efficiency (η_o) is the ratio of the amount of energy absorbed by the solar receiver and the amount of incidence solar energy on the solar collector's aperture, which depends on the optical properties of the material design, the geometry of the PTC, and the various imperfections arising from the construction of the PTC [1]. So, the η_o is the relationship of the reflectance of the reflector surface (ρ_r) for solar radiation, the transmittance of the glass enveloped tube (τ), the solar absorptance (α) of the solar absorber coated on the receiver tube, the intercept factor (γ), geometric factor (A_f), and the angle of incidence (θ). The η_o can be expressed as Eq. 7 [1, 2, 17].

$$\eta_0 = \rho_r \tau \alpha \gamma \left[\left(1 - A_f \tan\theta\right) \cos\theta \right] \tag{7}$$

The γ, defined as the ratio of energy intercepted by the receiver tube to the energy reflected by the parabolic reflector, depends on the receiver size, the errors of surface angle on the parabolic reflector, and the solar beam spread [1]. The A_f is expressed as the lost area divided by the aperture area. In this study, the geometry of the PTC and all the equipment was assumed to be perfect for the construction, thus, the γ, A_f, and θ were approximated to be 1°, 0° and 0° at normal incidence, respectively. So the term of $A_f \tan\theta$ in the Eq. 7 is equal to zero. The parameters, obtained from the thermal efficiency equation of the PTC using the three different coating thicknesses, are summarized in Table 2. The ρ_r and τ are the material properties of the flexible solar reflector and glass enveloped tube in this PTC construction. The α corresponds to the value of each Ni–Al coating thickness (Fig. 5). It is calculated that the η_o of all the thicknesses is identical, indicating that the η_o is independent of the thickness of Ni–Al coatings because they all have a similar α value. In addition, the η_o in this present study is close to those values of previous reports [2, 17]. The F_R significantly increases with increasing thickness of the Ni–Al coating and reaches 0.769 at the thickness of 299 μm, according to the increasing actual useful energy gain of the PTC. As for the slope of the line of all the thicknesses, the U_L significantly decreases with increasing coating thickness, meaning that the heat loss from the PTC to the surroundings is reduced. Looking at the results, increasing thickness of the Ni–Al coatings leads to an increasing F_R and a decreasing U_L in the thermal energy equation of the PTC. Among the three thicknesses, the Ni–Al coating with a thickness of 299 μm demonstrates the highest thermal performance. Therefore,

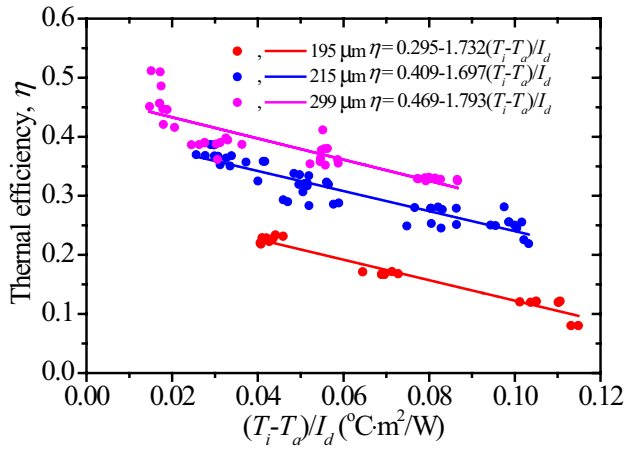

Fig. 8 The thermal efficiency of the PTC using the different thicknesses of Ni–Al coating on SS tube as solar absorber of receiver tube

Table 2 Summaries of the thermal performance parameters of the PTC, using the three thicknesses of Ni–Al coating on SS tube as solar absorber of receiver tube

Parameters	Thickness of Ni–Al coating		
	195 μm	215 μm	299 μm
Intercept ($F_R\eta_o$)	0.295	0.409	0.469
Slope ($-F_RU_L/C$)	1.732	1.697	1.793
ρ_r	90	90	90
τ	0.90	0.90	0.90
α	0.75	0.74	0.75
η_o	0.61	0.60	0.61
F_R	0.484	0.682	0.769
U_L	53.68	37.32	34.97

Table 3 Comparison of the thermal efficiency equation of this present study to previous reports

Researcher		Thermal efficiency equation
Kalogirou S. (1996) [18]		$\eta = 0.638–0.387\ (T_i - T_a)/I_d$
Valan Arasu and Sornakumar T. (2006) [23]		$\eta = 0.6905–0.3865\ (T_i - T_a)/I_d$
Valan Arasu and Sornakumar T. (2007) [17]		$\eta = 0.69–0.39\ (T_i–T_a)/I_d$
Xu L. et al. (2014) [22]		$\eta = 0.458–0.378\ (T_i–T_a)/I_d$
Valenzuela L. et al. (2014) [24]		$\eta = 0.768–0.0636\ (T_i–T_a)/I_d$
Kasaeian A. et al. (2015) [2]		$\eta = 0.6730–0.2243\ (T_i–T_a)/I_d$
Present study (Ni–Al solar absorber)	195 μm	$\eta = 0.295–0.1.732\ (T_i–T_a)/I_d$
	219 μm	$\eta = 0.409–1.697\ (T_i–T_a)/I_d$
	299 μm	$\eta = 0.469–1.793\ (T_i–T_a)/I_d$

the thermal performance of the PTC increases with increasing thickness of the Ni–Al coating.

These thermal efficiency equations of the PTC are compared with previous research works, as shown in Table 3. The current study's intercepts are mostly less than those of previous studies, except for the report of Xu L. et al. [22]. In the case of $-F_R U_L/C$ parameters, these values are greater than in previous studies. This indicates that the current study exhibits higher heat loss from the PTC to the surroundings. The thermal performance of this PTC is relatively low when compared with those equations in literature reviews, due to lower α of the solar absorber, lower direct solar irradiance (230 ± 30 W/m^2), the short length of the PTC (1 m), the simple construction of the PTC prototype, a rather high-pressure (4.3 kPa) inside the solar receiver tube of the PTC, and focusing errors due to the manual tracking system.

The Ni–Al coating prepared by the flame spray technique is a good candidate for a solar absorber for concentrating solar collectors, and it can be a guideline for developing solar absorber materials.

Conclusion

A Ni–Al coating of three different thicknesses was successfully prepared on the outer surface of a stainless steel 316L tube (SS tube) using a flame spray technique with Ni-5wt%Al powder as the starting material. SEM and EDX analyses of the cross-section area of the Ni–Al coating confirm that all three thicknesses consist of Ni, Al and O elements with a non-uniform chemical distribution. The O element distributes over the cross-sectional area of the sample and is predominantly in the Al-rich area. Ni, Al, NiO and Al_2O_3 phases are indexed on the Ni–Al solar absorber. The spectral R of all thicknesses are identical values over the whole wavelength range of UV–VIS-NIR and IR regions, indicating that the spectral selectivity of this coating is independent of its thickness. According to the thermal efficiency equation of the PTC based on the intercept ($F_R\eta_o$) and slope lines ($-F_R U_L/C$), the thermal performance of the PTC increases with increasing thickness of the Ni–Al coating, while the heat loss transfers from the PTC to the surroundings decreases. In conclusion, the Ni–Al coating prepared using the flame spray technique is a very promising candidate for a solar absorber material to use in concentrating solar collectors.

Acknowledgements This work was made possible by a generous grant from the National Research Council of Thailand (NRCT) through Naresuan University (Grant No. R2560B113), Phitsanulok, Thailand. The authors are also grateful to the Advanced Surface Technologies (AST) Co., Ltd., Ayutthaya, Thailand, for kindly providing flame spray equipment.

References

1. Kalogirou, S.A.: Solar thermal collectors and applications. Prog. Energy Combust. Sci. **30**, 231–295 (2004)
2. Kasaeian, A., Daviran, S., Azarian, R.D., Rashidi, A.: Performance evaluation and nanofluid using capability study of a solar parabolic trough collector. Energy Convers. Manag. **89**, 368–375 (2015)
3. Fernández-García, A., Zarza, E., Valenzuela, L., Pérez, M.: Parabolic-trough solar collectors and their applications. Renew. Sustain. Energy Rev. **14**, 1695–1721 (2010)
4. Antonaia, A., Castaldo, A., Addonizio, M.L., Esposito, S.: Stability of W-Al_2O_3 cermet based solar coating for receiver tube operating at high temperature. Sol. Energy Mater. Sol. Cells **94**, 1604–1611 (2010)
5. Selvakumar, N., Barshilia, H.C.: Review of physical vapor deposited (PVD) spectrally selective coatings for mid- and high-temperature solar thermal applications. Sol. Energy Mater. Sol. Cells **98**, 1–23 (2012)
6. Kennedy C. E., Review of mid- to high-temperature solar selective absorber materials *National Renewable Energy Laboratory (NREL)* (2002) 1–52
7. Rebouta, L., Pitães, A., Andritschky, M., Capela, P., Cerqueira, M.F., Matilainen, A., Pischow, K.: Optical characterization of

TiAlN/TiAlON/SiO_2 absorber for solar selective applications. Surf. Coat. Technol. **211**, 41–44 (2012)
8. Nuru, Z.Y., Arendse, C.J., Nemutudi, R., Nemraoui, O., Maaza, M.: Pt–Al_2O_3 nanocoatings for high temperature concentrated solar thermal power applications. Physica B **407**, 1634–1637 (2012)
9. Selvakumar, N., Manikandanath, N.T., Biswas, A., Barshilia, H.C.: Design and fabrication of highly thermally stable HfMoN/HfON/Al_2O_3 tandem absorber for solar thermal power generation applications. Sol. Energy Mater. Sol. Cells **102**, 86–92 (2012)
10. Hall, A., Ambrosini, A., Ho, C.: Solar selective coatings for concentrating. Adv. Mater. Process. **170**(1), 28–32 (2012)
11. Cai, F., Jiang, C.: Influences of Al particles on the microstructure and property of electrodeposited Ni–Al composite coatings. Appl. Surf. Sci. **292**, 620–625 (2014)
12. Dong, H.X., Jiang, Y., He, Y.H., Song, M., Zou, J., Xu, N.P., Huang, B.Y., Liu, C.T., Liaw, P.K.: Formation of porous Ni–Al intermetallics through pressureless reaction synthesis. J. Alloy Compd. **484**, 907–913 (2009)
13. Lee, H.Y., Ikenaga, A., Kim, S.H., Kim, K.B.: The effects of induction heating rate on properties of Ni–Al based intermetallic compound layer coated on ductile cast iron by combustion synthesis. Intermetallics **15**, 1050–1056 (2007)
14. Bunmephiphit, C., Suriwong, T., Jiajitsawat, S., Dejang, N.: Characterization of Ni–Al solar absorber prepared by flame spray technique. Key Eng. Mater. **675–676**, 477–481 (2016)
15. Katumba, G., Olumekor, L., Forbes, A., Makiwa, G., Mwakikunga, B., Lu, J., Wäckelgård, E.: Optical, thermal and structural characteristics of carbon nanoparticles embedded in ZnO and NiO as selective solar absorbers. Sol. Energy Mater. Sol. Cells **92**, 1285–1292 (2008)
16. Gueymard, C.A.: The sun's total and spectral irradiance for solar energy applications and solar radiation models. Sol. Energy **76**, 423–453 (2004)
17. Arasu, A.V., Sornakumar, T.: Design, manufacture and testing of fiberglass reinforced parabola trough for parabolic trough solar collectors. Sol. Energy **81**, 1273–1279 (2007)
18. Kalogirou, S.: Parabolic trough collector system for low temperature steam generation: design and performance characteristics. Appl. Energy **55**, 1–19 (1996)
19. Xu, C., Du, L., Yang, B., Zhang, W.: The effect of Al content on the galvanic corrosion behaviour of coupled Ni/graphite and Ni–Al coatings. Corros. Sci. **53**, 2066–2074 (2011)
20. Sampath, S., Jiang, X.Y., Matejicek, J., Prchlik, L., Kulkarni, A., Vaidya, A.: Role of thermal spray processing method on the microstructure, residual stress and properties of coatings: an integrated study for Ni-5 wt%Al bond coats. Mater. Sci. Eng. A **364**, 216–231 (2004)
21. ASHRAE Standard 93-1986 (RA 91). In: *Methods of testing to determine the thermal performance of solar collector*, American Society of Heating, Refrigerating, and Air-Conditioning Engineers, Atlanta, GA (2002)
22. Xu, L., Wang, Z., Li, X., Yuan, G., Sun, F., Lei, D., Li, S.: A comparison of three test methods for determining the thermal performance of parabolic trough solar collectors. Sol. Energy **99**, 11–27 (2014)
23. Arasu, A.V., Sornakumar, T.: Performance characteristics of parabolic trough solar collector system for hot water generation. Int. Energy J. **7**, 137–145 (2006)
24. Valenzuela, L., López-Martín, R., Zarza, E.: Optical and thermal performance of large-size parabolic-trough solar collectors from outdoor experiments: a test method and a case study. Energy **70**, 456–464 (2014)